Key Lessons from a Modeling and Migration Experiment

John Bancroft*
University of Calgary, Calgary, AB
bancroft@ucalgary.ca

and

Hesham Moubarak and Don Lawton
University of Calgary, Calgary, AB, Canada

Summary

Two dimensional (2D) forward numerical seismic modeling of a complex geology structure was used to optimize the acquisition parameters, to evaluate processing techniques, and to aid in the seismic interpretation. Synthetic seismic data were acquired using a numerical model of a fault-fold structure encountered in northeastern British Columbia. These gathers are used to investigate which migration algorithms would produce the best images in such complex environments. Pre-stack depth migration from the topography with the known velocity model was found to give the optimum migrated image. Acoustic and elastic numerical modeling techniques were used to simulate waves propagating in the complex medium but only the acoustic results are shown here.

A near vertical structure that was difficult to image was chosen for a comprehensive analysis. This seismic structural imaging investigated the target locations in the Husky line, Muskwa region. The line is severely affected by the harsh topography, velocity variations and complex geometry that cause severe ray bending. Prestack time migration (PreSTM) cannot handle the lateral velocity variations and the severe ray bending introduced by such complex geometry. It caused deterioration of the image that poses problems for interpretation. To alleviate this problem, we used an isotropic Kirchhoff prestack depth migration (PreSDM) (from TESSERAL modeling and migration software) incorporating the exact velocity model. Traveltimes for the Kirchhoff migrations were computed using both the first-arrival times as well as maximum-energy arrival times. The maximum energy arrival times produced a superior image.

Introduction

Information from the well logs and the surface geology were combined to begin constructing the geological model. The model is fully-balanced in which the areas of layers are preserved. The balancing and restoration of this model was an important step to test the viability of geological interpretation of a Husky line, especially for the geometrical validity of interpreted fault and associated faulted strata, allowing constraints to be placed on interpretation and giving a more geometrically accurate geologic model.

The first model was created on a set of surfaces derived directly from the seismic interpreted section; the 2D wavefront propagation contained an excessive number of wavefronts. The total area

of the wavefronts increased considerably during propagation, leading to a larger number of waves. A major part of the computation is related to the wavefront propagation in areas where the velocity is more complex, particularly across interfaces. Therefore, the computation time and disk space requirements increase dramatically. In order to improve the quality of the model and the speed of computation, a new velocity field was created using well log information.

Several iterations were made before the final model was built and the velocities and densities of the formation units inserted. The final model, showing only the P-wave velocities, is shown in Figure 1.

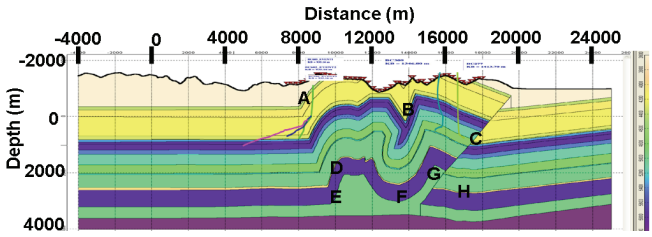

Figure 1: Balanced full geologic model with the eight target zones are identified by (A-H) showing the complete lateral extent, scaled one-to-one vertical scale matching the horizontal scale. Drilled wells are superimposed on this model. This Husky model geometry includes high velocity bodies (in blue and purple) embedded in a lower velocity

The modeling process begins with an analysis of the velocity and the interpreted surfaces in the target zones (A: Box-fold of Gething Formation B: central syncline of Fernie Formation, C: fault plane, D: Box-fold of both Golata and Debolt Formations, E: Box-fold of Banff, F: syncline of Debolt, G: hinge of Debolt, H: shadow zone beneath the fault plane) which for simplicity are shown on the final model in Figure 1. The complete lateral extent is scaled one-to-one with the vertical scale matching the horizontal scale. Our initial interest is in the steep box-fold in the areas of D and E in Figure 1.

This model represents different structural styles that might influence trapping mechanisms and reservoirs.

Ray Tracing

Normal incident rays were traced from all the horizons to establish the source locations and the recording time required to record the energy from problem areas. Establishing the source location, where the normal incident rays reach the surface, ensures a range of offsets will record from the problem areas.

Seismic Illumination

Wave equation modeling was used in this experiment. From this type of modeling, the amplitudes of the energy distribution throughout the structure can be estimated. Examples of the energy distribution from two different source locations are shown in Figure 2. The refraction of energy produces areas with good and poor illumination through different parts of the subsurface. In a homogeneous medium, the illumination would appear as expanding circles of different colors.

Monitoring areas with poor illumination contributes to the field design by placing more effort at different surface locations.

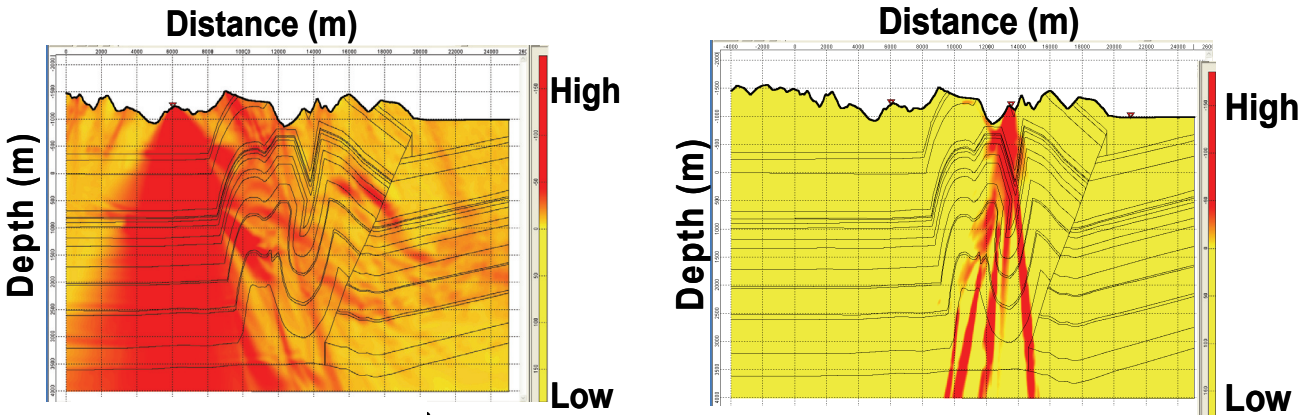

(a) (b)

Figure 2: (a) Good and (b) poor Illumination.

Wavefront Propagation

Energy from one source location is then tracked through the model. Snapshots of the energy are created at four millisecond intervals, and the energy arriving at the surface is recorded as a line of energy in the source record. Four seconds of recorded data will require one thousand snapshots to be created. Figure 3 shows only three of these snapshots. It is then possible to track the downward propagating energy to reflection areas that produce poor imaging. The reflected energy can then be followed to the surface, and then identified on the synthetic source record. Figure 3 shows the wavefront propagation of a source at location 6000m. Three snapshots at 1250 ms, 1500 ms, and 1750 ms are used to identify the energy reflected from the Debolt Formation.

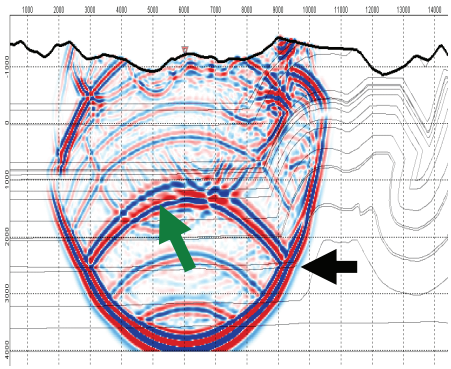

a) Snapshot at 1250 ms.

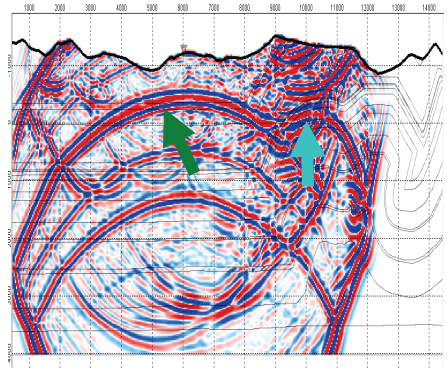

b) Snapshot at 1500 ms

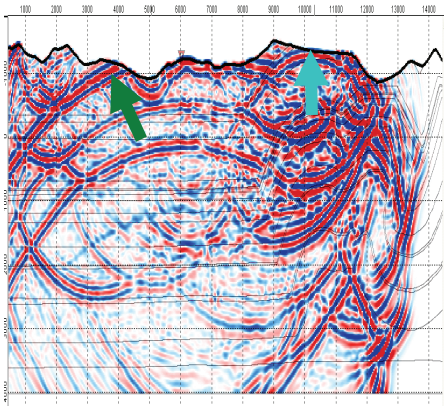

c) Snapshot at 1750 ms

Figure 3: Wavefield recorded at times a) at 1250 ms, b) at 1500 ms, and c) at 1750 ms. The energy at the surface is mapped at these times to the source record in Figure 4.

Energy, reflected from the horizontal portion of the Debolt formation (identified by the black arrow), can be observed rising toward the surface in a semi-circular shape at the location of the green arrow.

The wavefront is also just arriving at the box fold portion of the Debolt near the location of the black arrow. The steep part of this structure is difficult to image, however the upper more rounded portion is easier to image. In the snapshot at 1500 ms of Figure 3b, the horizontal reflection progresses to the surface along with the energy from the upper portion of the fold identified by the blue arrow. Note how this energy tapers off to the left. It is these weak amplitudes that contain the reflection information of the steeper part of the box fold. In Figure 3c, at a time of 1750 ms, the energy has arrive at the surface and is mapped to the source record, as identified by the red line in Figure 4.

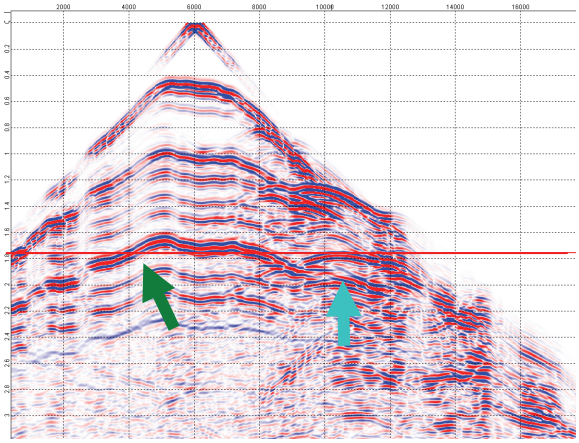

Figure 4: The source record at location 6000 m. It is composed from 800 wavefield snapshots.

Energy from the Debolt Formation, both from the horizontal reflector and the folded portion, can be observed on the source record around the time of 1750 ms. The curvilinear nature of this reflection is due to the rugged surface as observed in the snapshots.

The weak energy from the steeper portion of the fold appears to taper to zero and will not be able to image the steepest portion. This problem is further emphasized by the illumination diagram in

Figure 5. Note that refraction is focusing energy to the upper part of the fold, identified by the blue ellipse, and is weaker in the steeper portion, identified by the red ellipse.

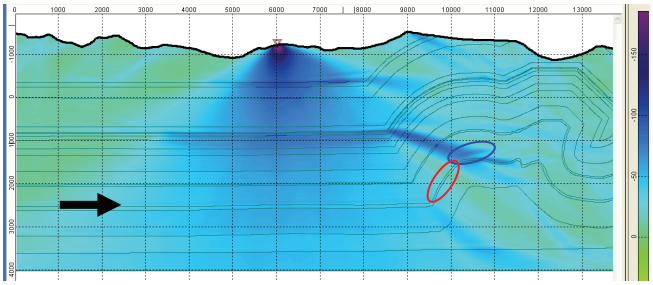

Figure 5: Illumination diagram for the source record at the location 6000m over lying the geological structure.

Migrations

A prestack Kirchhoff depth migration of the above source record is shown in Figure 6. There is reasonable reconstruction of the horizontal formations, especially in the presence of the rugged surface. However, there is an absence of the steeper dips.

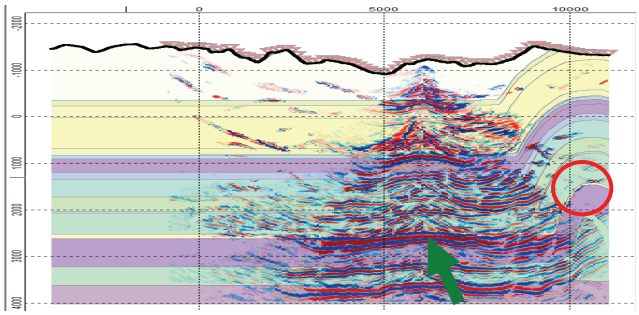

Figure 6: Prestack Kirchhoff depth migration of the source record. Energy is missing from the migration.

The algorithm used appears to have a dip limit that prevents the reconstruction of the dipping energy, even though part of it was recorded.

Complete migrations of the data in this area are shown in Figures 7 and 8. Both are prestack Kirchhoff depth migrations, but the difference is in defining the traveltimes. They both used wave propagation to compute the traveltimes, but the first used the first arrival traveltimes, while the second used the arrival times of the maximum energy. In addition, the data in Figure 8 used longer offsets and more source locations to the left. It should be noted that the parameter selection of both migrations could be modified to improve the imaging, especially of the steeper dipping events.

Conclusions

TESSERAL modeling software is a robust tool that helps construct models, creates snapshots of the energy wavefronts, builds source records, and migrates the data. The software enabled clipping of the amplitudes displayed in the snapshots that allowed the display and tracking of the weak reflection energy.

A procedure was described that helped define acquisition parameters, traced energy from difficult imaging areas to source records, and then to migrated sections.

2D prestack Kirchhoff depth migration using maximum energy traveltime yielded the best result for imaging steeper dips.

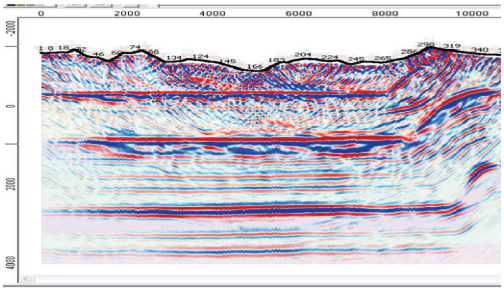

Figure 7: Prestack Kirchhoff depth migration using first arrival traveltimes.

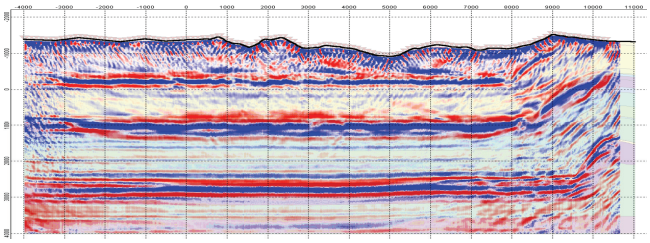

Figure 8: Prestack Kirchhoff depth migration using longer offsets and maximum energy traveltimes.

Acknowledgements

We would also like to thank the sponsors of CREWES (Consortium for the Research in Elastic Wave Exploration Seismology), and the sponsors of FRP (Fold-Fault Research Project) for supporting this work, and TESSERAL for providing access to the modeling and imaging software used.

Special thanks to Larry Newport, and David Emery of Husky Energy for providing the Husky data and for the financial assistance.